DOI: 10.1070/RCR4633

Third-generation solar cells based on quaternary copper compounds with the kesterite-type structure

Vladimir V. Rakitin, Gennady F. Novikov

Institute of Problems of Chemical Physics, Russian Academy of Sciences
prosp. Akademika Semenova 1, 142432 Chernogolovka, Moscow Region, Russian Federation

The state of the art in the studies aimed at improving the efficiency and reducing the cost of solar energy cells is analyzed. A possible way to achieve these goals is to use absorber layers made of semiconductor materials based on a new, poorly studied class of quaternary copper compounds Cu_2ZnSnX_4 (X = S, Se) with the kesterite-type structure. Methods of synthesis and the chemical composition of the kesterite absorber layers are discussed. Various types and operating principles of thin-film solar cells as well as main factors influencing parameters of these devices are considered.
The bibliography includes 173 references.

Contents

I. Introduction 99
II. Kesterite thin films in solar photovoltaics 100
III. The structures of kesterite and stannite 102
IV. Electrophysical and optical properties of kesterite materials 105
V. Solar cells based on CZT(S,Se) kesterite films 107
VI. Conclusion 108

I. Introduction

In the last decade, there has been intensive research into various types of solar energy cells and, in particular, thin-film solar cells based on quaternary copper compounds Cu_2ZnSnX_4 (X = S, Se) and solid solutions $Cu_{2-x}Zn_{2-y}Sn_yS_{4-z}Se_z$ ($0 < x$, $y < 2$, $0 \leqslant z \leqslant 4$) with the kesterite-type structure built of naturally abundant elements. In the literature, these compounds are designated by CZT(S,Se). They are low-toxic, which facilitates disposal of spent solar cells. It is important that many properties of CZT(S,Se) films are similar to those of $Cu(In,Ga)Se_2$ films (they are designated by CIGS); solar cells based on the CIGS films exhibit the highest power conversion efficiency (PCE) among all types of thin-film solar cells.[1]

Owing to higher natural abundance and lower toxicity of zinc and tin compared with gallium and indium, kesterites CZT(S,Se) are thought to become a promising alternative to CIGS.[2,3] This type of materials belongs to direct band-gap semiconductors with a band gap, E_g, of 1.5 (CZTS) and 1.0 eV (CZTSe), which meets the requirements for photovoltaic solar energy converters. The band gaps of sulfide – selenide compositions $Cu_2ZnSnS_{4-x}Se_x$ ($0 < x < 4$) lie between 1 and 1.5 eV.

Katagiri *et al.*[4] pioneered in the studies of a CdS/CZTS photovoltaic heterojunction with a PCE of less than 0.7%. Since then the CZT(S,Se) materials have been discussed as promising candidates for thin-film solar cells; probably, they are the future of thin-film photovoltaics of the 21st century.

In the last decade, a number of reviews on the design of advanced CZT(S,Se) semiconductor materials for thin-film photovoltaics have been reported.[5–10] However, some of them only concern various methods of synthesis of the materials, whereas other reviews are dedicated to application of kesterite absorber layers in thin-film solar cells and relevant methods of synthesis. The most complete information on kesterites was collected in Refs 9 and 10; however, new data became available since then.

It should be noted that the most appropriate method of synthesis of CZT(S,Se) absorber layers is unknown; the reasons for significant differences between the experimentally achieved PCE of the solar cells based on CZT(S,Se) and theoretically possible values are still to be clarified; also, the defect structure and the presence of secondary phases in the kesterite films as well as their influence on the optical and electrophysical properties of CZT(S,Se) com-

V.V.Rakitin Candidate of Chemical Sciences, Researcher at the IPCP RAS.
Telephone: +7 (496) 522 – 1842, e-mail: domi-tyan@yandex.ru
G.F.Novikov Doctor of Physical and Mathematical Sciences, Head of Laboratory of Photoelectrophysics at the IPCP RAS and Professor at the Lomonosov Moscow State University.
Telephone: +7 (496) 522 – 1842, e-mail: ngf@icp.ac.ru
Current research interests of the authors: solar cells, synthesis of advanced thin-film materials and studies on their electrophysical properties.

Received 4 February 2015
Translation: A.M.Raevskiy

© 2017 Russian Academy of Sciences and Turpion Ltd.

pounds remain debatable and unclear. Moreover, solar cells based on kesterites are not industrially produced as yet.

The review is concerned with a particular type of solar cells, namely, thin-film solar cells based on Cu_2ZnSnX_4 (X = S, Se) semiconductor absorber layers with the kesterite-type structure. This avenue of research in modern photovoltaics is rapidly progressing, still being in the early stage of development. Published data on the methods of synthesis and on the influence of the secondary phases and defect structure on the properties of kesterite films are generalized and possible reasons for short lifetimes of charge carriers and, as a consequence, low PCE of the solar cells based on CZT(S,Se) absorber layers are discussed.

We also outline changes in the character of recent activity in the design of thin-film solar cells, namely, an important role of kinetic studies, numerical simulation of processes, analysis of the role of the elemental concentration gradients in the films, inter-grain boundaries, influence of the band gap, *etc*. Research into these subtle aspects has become possible owing to the emergence of new experimental methods.

II. Kesterite thin films in solar photovoltaics

II.1. The minerals kesterite and stannite

The CZT(S,Se) compounds are named after kesterite,† a mineral from the stannine family. Kesterite is an opaque, green-black or black mineral with the composition $Cu_2(Zn,Fe)SnS_4$. Its density lies in the range from 4.54 to 4.59 g cm^{-3}. Isometric kesterite crystals belong to the tetragonal crystal system, can be as large as a few centimetres and can form irregular grains and large aggregates. The mineral occurs in hydrothermal quartz-sulfide veins at tin deposits. The mineral stannite has the composition Cu_2FeSnS_4. Its crystals also belong to the tetragonal crystal system, but the space groups of kesterite and stannite are different. Stannite contains small amounts of zinc, whereas the Zn : Fe ratio for kesterite much exceeds that for stannite.

II.2. The properties of kesterite layers: a comparison

Currently, silicon-based solar cells are used most widely. However, they have a number of severe drawbacks due to intrinsic properties of crystalline silicon, in particular, a relatively large film thickness ($\sim$200 μm) and, as a consequence, poor mechanical properties of the devices. Silicon-based solar cells have almost reached their potential, namely, commercially available samples are characterized by PCE $\approx$ 17%.[14–17] Further improvement of their efficiency requires expensive ultrahigh-purity silicon. Solar cells based on amorphous silicon also have an efficiency threshold. Also, hydrogen present in the silicon structure favours manifestation of negative Staebler–Wronski effect (light-induced degradation of physical properties).[16, 18]

Solar cells based on gallium arsenide represent an alternative to silicon photocells. Gallium arsenide, a semiconductor whose solar-power properties are identical to those of silicon, is more efficient from the standpoint of performance. That is why GaAs-based solar cells have a much higher PCE of up to 44%, outside the Earth's atmosphere.[16] However, this type of solar cells is used more rarely, mainly in specialized industries (*e.g.*, space industry) because of very high cost of the devices (this is their main drawback). Both the material and fabrication technology are much more expensive than those of the silicon analogues. Besides, gallium is quite a rare metal.[3, 16, 19]

In this connection, other technologies including thin-film ones are intensively developed. They are used to prepare solar cells based on CdTe, CIGS and, of course, CZT(S,Se) thin films.[3, 16, 19, 20] [Note that CdTe-based solar cells rank second worldwide in production volume ($\sim$25%) after silicon-based devices.] Solar cells based on CdTe are characterized by PCE values of about 10%–12% and cheap fabrication technology. High toxicity of cadmium and relatively low natural abundance of tellurium preclude‡ large-scale production of CdTe-based solar cells in many countries.[16, 19]

Devices based on CIGS films have PCE > 12% and are in the commercialization process. However, they contain rare expensive elements, indium and gallium.[1, 16] In this connection, a possible alternative to CIGS is to use quaternary copper compounds CZT(S,Se) (kesterites) that have been studied quite recently. They have an optimal band gap ($E_g \approx 1.0-1.5$ eV), high absorption coefficient ($\alpha \approx 10^4$ cm^{-1}), and almost complete absorption of solar radiation is provided with a layer nearly 3 μm thick ($\delta \approx 3$ μm). Also, the constituent elements of kesterites are low-toxic and abundant in nature. However, the PCE of the solar cells based on CZT(S,Se) is at most 13%, being much lower than the theoretically possible value of 30%.[2–5] The reasons for this difference have been poorly studied as yet.[22–25] Also, no industrial-scale production of this type of solar cells is currently available.

The CZT(S,Se) semiconductor materials have hole-type conductivity. The concentration of current carriers in them lies in the range $10^{18}-10^{20}$ cm^{-3} (see Refs 3, 26–30). The Hall mobility of holes (μ_H) depends strongly on the method of synthesis (Table 1). A maximum Hall mobility of 120 cm^2 V^{-1} s^{-1} was reported for magnesium-doped samples.

† The mineral was discovered at the Kester deposit (Arga-Ynnakh-Khaya granite massif, Yana-Adycha Region, Yana River Basin, Yakutia/Sakha Republic, Russian Federation). It was first described in 1948 as 'silver zinc stannite' despite the fact that the silver content was only 0.005%. The mineral was named 'kesterite' in 1956.[11–13]

‡ However, First Solar, Inc. (USA) has been producing this type of modules since 1990s and has no plans to change the strategy.[21]

Table 1. The Hall mobility of holes.

Compound	μ_H /cm^2 V^{-1} s^{-1}	Ref.
Cu_2ZnSnS_4	6.3	31
Cu_2ZnSnS_4	6.0	30
Cu_2ZnSnS_4	<0.1	32
Cu_2ZnSnS_4	12.6	33
$Cu_2ZnSnSe_4$	39.7	34
$Cu_2ZnSnSe_4$	36.5	35
$(Cu_{2-x}Mg_x)ZnSnSe_4$	120	35
$Cu_{1.75}Zn(Sn_{1-y}Al_y)Se_4$	32.5	36
$Cu_{1.6}Zn_{1+z}Sn_{1-z}Se_4$	113	37
$Cu_2ZnSnSe_4$ (single crystal)	40–50	38

Table 2. Absorber layers of industrially produced one-cascade solar cells: a comparison.

Absorber layer	Advantages	Drawbacks	Ref.
Si (crystalline)	PCE > 25%	$\delta \approx 200$ μm, expensive technology, brittle	14 – 17, 39
Si (amorphous)	PCE > 10%; $\alpha > 10^5$ cm^{-1} ($\delta \approx 0.5 - 1.0$ μm)	Staebler – Wronski effect (a decrease in PCE by 5% every 6 months)	16, 18, 40
GaAs	PCE ≈ 30%; $\delta \approx 1$ μm	Expensive substrates, brittle, toxic element As	3, 16, 19, 41
CdTe	PCE to 21%; cheap	Toxic element Cd and rare element Te	16, 19 (see [a])
CIGSe	PCE to 21%; low-toxic; $\delta \approx 2 - 3$ μm	Rare and expensive elements In and Ga	1, 16 (see [b])
Cu_2ZnSnX_4 (X = S, Se)	PCE of laboratory-scale samples to 12.6%; cheap; $\delta \approx 2 - 3$ μm; low-toxic	No industrial-scale production	2 – 5, 42

[a] See also First Solar Press Release, 'First Solar Builds the Highest Efficiency Thin Film PV Cell on Record', 5 August 2014. (http://investor.firstsolar.com/releasedetail.cfm?ReleaseID = 864426).
[b] See also Solibro Press Release, 'Solibro Beats World Record for Solar Cells', 12 June 2014. (http://www.zsw-bw.de/uploads/media/pr12-2014-ZSW-WorldrecordCIGS.pdf).

Key properties (PCE, thickness) and the advantages and drawbacks of the absorber layers for industrially produced one-cascade solar cells are compared in Table 2.

II.3. Main methods of synthesis of kesterite thin films

Kesterite thin films Cu_2ZnSnX_4 (X = S, Se) are most often synthesized using vacuum and solution methods.

Kesterite absorber layers can be synthesized using various methods including atom-beam sputtering,[32, 43] hybrid sputtering,[30] radiofrequency magnetron sputtering,[44] thermal evaporation,[45] pulsed laser deposition,[46, 47] electron-beam evaporation of precursors followed by treatment in sulfur (or selenium) vapours,[4, 48] as well as using spray pyrolysis,[49, 50] sol – gel technology,[51, 52] *etc*. These methods require expensive precursors and complex equipment. In some cases, toxic side products are formed. Also, usually one should work at high temperatures, which favours interdiffusion of the constituent elements and significant degradation of the quality of the thin-film solar cell structure.[53] Some features of these methods of synthesis are described in more detail in the literature.[6, 54, 55]

II.3.a. Vacuum methods

Currently, vacuum methods of synthesis are most often used, because they allow one to prepare thin films of specified composition and, hence, to study particular aspects using model systems and compare the properties of the films. Generally, a vacuum synthesis at $T = 500 - 550$ °C can be described by the following equation:

$$2\,Cu + Zn + Sn + 4\,S \longrightarrow Cu_2ZnSnS_4 \qquad (1)$$

The process begins with successive deposition of metals onto a substrate and then the film is annealed in sulfur (or selenium) vapours or in a hydrogen sulfide (or hydrogen selenide) atmosphere.

Precursors can be deposited in different regimes in order to assess how the order of deposition of constituent elements and the defect structure or the concentration gradient of a certain element in the film influence the electrophysical and optical properties of the film as well as the properties and performance of the whole solar cell.[56 – 59]

Two main kinds of vacuum methods include thermal evaporation of elements and d.c. or a.c. magnetron sputtering of targets. Copper, zinc and tin were either successively deposited or co-deposited onto substrates[60 – 62] to give stacks, which were subsequently annealed in the reactive atmosphere of sulfur or selenium (or in a hydrogen sulfide or hydrogen selenide flow) at ~500 – 550 °C to form the final CZT(S,Se) structure. This made it possible to assess the effect of the order of deposition of components and that of substrate temperature; however, annealing of stacks can be accompanied by the loss of some elements (*e.g.*, Zn, Se, S) and intermediates (SnS, SnSe) through their sublimation. This will influence the final chemical composition of the films.

The problem can be partially solved using intermetallics or binary sulfides and metals as precursors.[63] This operating regime decreases the loss of elements from CZT(S,Se) films. Examples are provided by the following reactions:[63, 64]

$$[Cu_2S + SnS]_{(liq)} + ZnS + S_{2(gas)} \xrightarrow{> 480\ ^\circ C} Cu_2ZnSnS_4 \qquad (2)$$

$$0.17\,Cu_6Sn_5 + 0.096\,Cu_5Zn_8 + 0.382\,Zn + 4\,S \xrightarrow{550\ ^\circ C} Cu_{1.5}Zn_{1.15}Sn_{0.85}S_4 \qquad (3)$$

Radiofrequency d.c. and a.c. sputtering of targets onto glass substrates is also a convenient method for the preparation of CZT(S,Se) thin films. Numerous studies on successive deposition of constituent elements from monometallic targets[65 – 67] and from multi-element targets[68 – 70] followed by annealing are available. In the latter case, one-step precursor film deposition is possible, which reduces the synthesis time. Also, combining radiofrequency sputtering and thermal evaporation of elements allows the mechanism of formation of CZT(S,Se) films of different composition to be studied in more detail.[71, 72]

Optimization of conditions for thin-film vacuum deposition in the last decade made it possible to improve the PCE of thin-film solar cells based on CZTS from 0.66 (Ref. 4) to 6.8%.[73, 74] However, exact chemical composition of CZT(S,Se) films corresponding to the maximum PCE of solar cells based on these films remains unknown.

II.3.b. Solution methods

The advantages of solution methods over vacuum ones are as follows:[75 – 78]

— practical implementation of solution methods is much cheaper;

— operation at ambient temperatures;

— operation with large-surface-area substrates of arbitrary shape; and

— favourable working conditions.

Solution methods include first of all chemical bath deposition (CBD) of precursor films onto various substrates.[79–84] This allows one to study the mechanisms of formation of colloidal nanoparticles and nanocrystalline kesterite precursor films in the course of adsorption of elements from solution to the substrate and to form the film during the chemical reaction between the deposited elements using additional annealing in a reactive sulfur- or selenium-containing atmosphere.

Solution methods include, in particular, two versions of electrochemical deposition, namely,

— successive galvanic coating and

— one-step electrochemical deposition.

In the former case, one deals with successive electrochemical deposition of metals and formation of a Cu–Zn–Sn precursor film[85–88] in an electrolyte bath followed by sulfurization or selenization [see reaction (1)] at specified temperatures (~500–550 °C) resulting in the CZT(S,Se) film. The method assumes the use of particular solutions to deposit each metal; this extends the synthesis time. However, the advantage of the technique consists in the possibility of studying the influence of the order of deposition of components and the possibility of alloying in the course of deposition.

In the latter case, all four components are simultaneously deposited from the same working solution. Examples are provided by the electrochemical deposition of components from the same solution at a common potential:

$$Cu^{2+} + 2e \longrightarrow Cu^0 \quad (4)$$

$$Zn^{2+} + 2e \longrightarrow Zn^0 \quad (5)$$

$$Sn^{2+} + 2e \longrightarrow Sn^0 \quad (6)$$

$$S_2O_3^{2-} + 6H^+ + 4e \longrightarrow S^0 + 3H_2O \quad (7)$$

and low-temperature formation of a precursor film

$$Cu^0 + Zn^0 + Sn^0 + S^0 \longrightarrow Cu-Zn-Sn-S \quad (8)$$

Next, high-temperature (T = 500–550 °C) annealing in inert or reactive atmosphere is carried out to give Cu_2ZnSnS_4. The method enables operation with only one solution, thus making the preparation of precursor films faster, and simplifies regeneration of the working solution.

Although there are few studies on one-step electrochemical deposition of CZT(S,Se) thin films, mention may be made of some advances in the synthesis of the kesterite CZTSe.[89,90] Also, attempts were made to prepare CZTS thin films from a buffer solution containing citrate and tartrate ions.[88,91–94] However, the system appeared to be unstable and long-term used of the solution can result in the formation of stable tartrate deposits. This reduces the reproducibility of experimental results. Besides, annealing was performed in the atmosphere containing no sulfur, which also influenced the final film composition and the films thus prepared were multiphase and contained large amounts of impurities; this could be determined with ease by powder X-ray diffraction. It was proposed to fabricate CZTS thin films by one-step electrochemical deposition of precursors from a stable citrate buffer solution followed by annealing in a sulfur atmosphere.[95] It was found that the CZTS thin films thus synthesized contained no secondary phases and were photoactive.

However, in spite of some advances in the field, solution methods of synthesis of CZT(S,Se) thin films are almost not used in the Russian Federation.

III. The structures of kesterite and stannite

III.1. The crystal lattices of kesterite and stannite

Two main structure types of the compounds $A^I_2B^{II}C^{IV}X^{IV}_4$ are the kesterite-type structure and the stannite-type structure (Fig. 1).[3,96–101] Both of them belong to the tetragonal crystal system and comprise an anionic matrix and cations occupying 50% of structural voids. Thus, the two structures are interrelated but belong to different space groups because of different distributions of the cations A^+, B^{2+} and C^{4+}. Compounds CZT(S,Se) crystallize in the kesterite-type structure. Hall *et al.*[99] reported an ordered cation distribution, whereas Schorr and co-workers in a neutron powder diffraction study[13] revealed a disorder of cations in the Cu–Zn layer in positions 2*c* and 2*d*. Initial calculations for CZTS predicted a kesterite-type structure with *I*4 symmetry as the most stable, probably, owing to cation disorder in the Cu–Zn layer.

It was shown that CZTSe can crystallize in the stannite-type structure with Zn^{2+} cations occupying position 2*a* and Cu^+ cations occupying position 4*d*.[102] Based on the results of the initial calculations,[103] it was assumed that compounds $A^I_2B^{II}C^{IV}X^{IV}_4$ with the kesterite-type structure are more stable than those with the stannite-type structure. The latter was reported in the literature (see, *e.g.*, Ref. 102) as the most probable owing to the disorder in the A–B layer of the kesterite-type structure. A comparison of the experimental and calculated crystal structures of the quaternary compounds $A^I_2B^{II}C^{IV}X^{IV}_4$ showed that this is incorrect.[103] Structure refinement remains topical because of the need for exact description of the chemical and physical properties of these compounds as well as for their applications as absorber layers in thin-film solar cells. Additional information on the structure of kesterites can be found in the literature.[104–107]

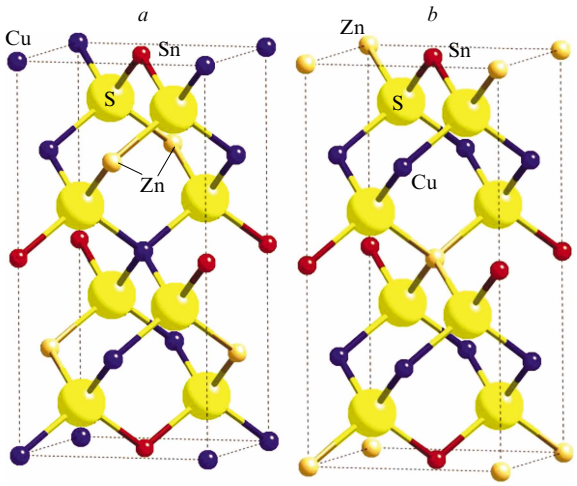


Figure 1. Crystal lattices of kesterite (*a*) and stannite (*b*) with different positions occupied by copper and zinc atoms.[96]

III.2. Phase composition, as determined from powder X-ray diffraction data

Kesterite films CZT(S,Se) are polycrystalline, being mainly identified by powder X-ray diffraction. The main lines in the X-ray diffraction patterns of the CZT(S,Se) films with the kesterite-type structure are near $2\theta = 28^\circ$ (112), 47° (220) and 56° (312) (Fig. 2).[63, 65, 67, 72, 92, 95] Since the main lines in the X-ray diffraction patterns of a number of binary (ZnS, ZnSe, *etc.*) and ternary (Cu_3SnS_4) compounds are observed at the same 2θ values, the kesterite-type structure cannot be unambiguously identified based only on the powder X-ray diffraction data.[13] Besides, the method is low sensitive to small amounts of secondary phases, which also precludes unambiguous conclusion of the single-phase composition of the film prepared.

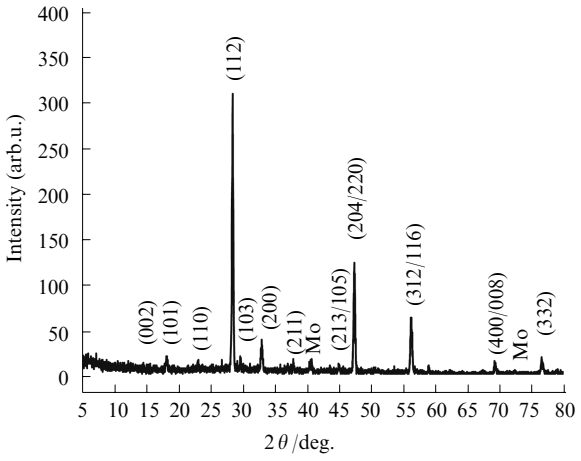


Figure 2. X-ray diffraction pattern of a CZTS film sample prepared by magnetron sputtering of metallic targets followed by annealing at 550 °C in hydrogen sulfide atmosphere.[65]

III.3. Raman spectroscopy, as a method for identification of the kesterite-type structure

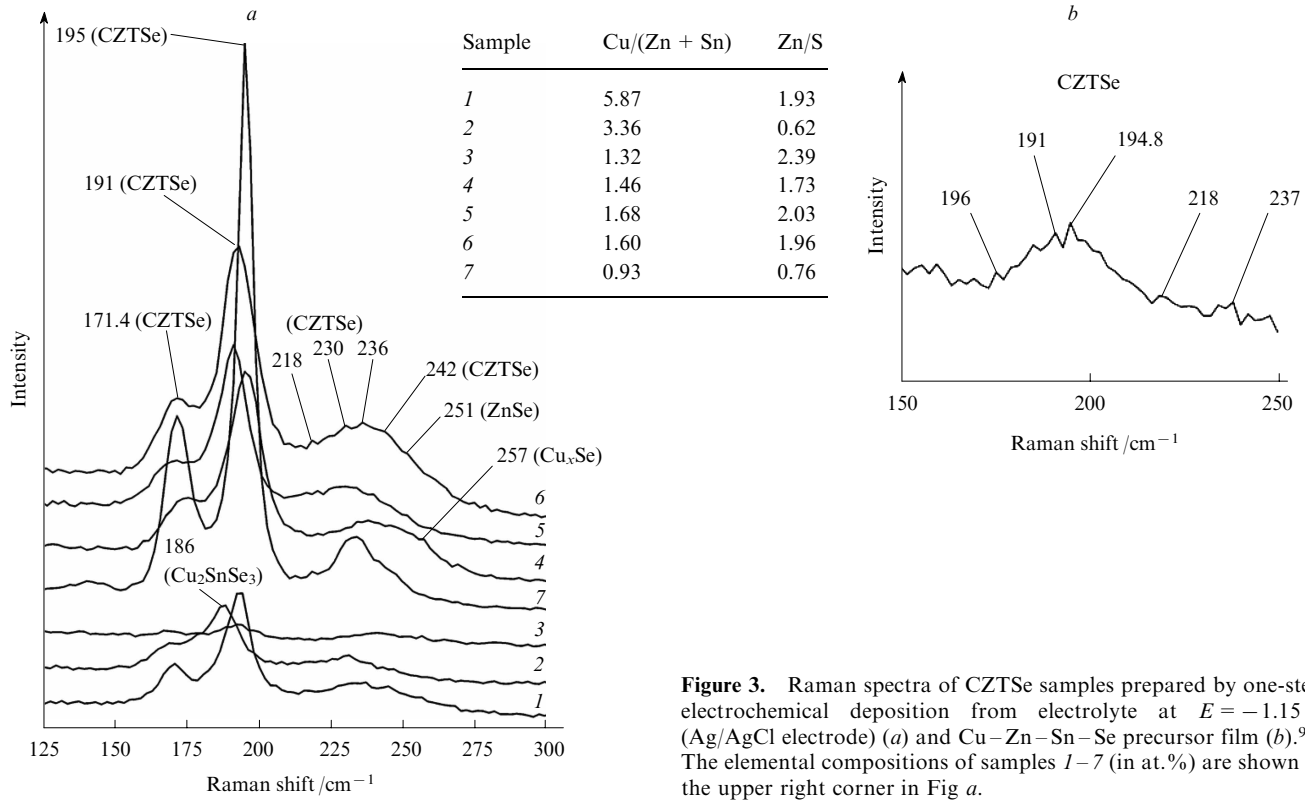
Raman spectroscopy is used as additional method of analysis. Vibrational spectroscopy provides fundamentally important information on the molecular structure and on the type of chemical bonds between molecules. Positions of the characteristic peaks (in cm^{-1}) are as follows:

— for Cu_2ZnSnS_4 — 288 – 289, 338 – 339, 351, 368 – 373;

— for $Cu_2ZnSnSe_4$ — 171 – 173, 194 – 196, 230 – 231, 390.

These peaks were reported as 'fingerprints' of the CZT(S,Se) thin films with the kesterite-type structure.[71, 72, 89, 91, 93] The presence of these peaks in the spectrum confirms the presence of a compound whose films have the kesterite-type structure. As an example, Fig. 3 presents the Raman spectra of the CZTSe samples prepared by one-step electrochemical deposition from an electrolyte at $E = -1.15$ V (Ag/AgCl electrode).[90] As can be seen, position of the peaks of the secondary phases (Cu_2SnSe_3 at 186 cm^{-1}, ZnSe at 251 cm^{-1} and Cu_xSe at 257 cm^{-1}) differ from those of the peaks of the kesterite phase (main peaks are near 195 and 171.4 cm^{-1}), which allows one to clearly identify the structures formed and to control the amount of the secondary phases in the final film.

The main Raman lines of all possible phases that can form during the synthesis of CZT(S,Se) thin films are listed in Table 3.



Sample	Cu/(Zn + Sn)	Zn/S
1	5.87	1.93
2	3.36	0.62
3	1.32	2.39
4	1.46	1.73
5	1.68	2.03
6	1.60	1.96
7	0.93	0.76

Figure 3. Raman spectra of CZTSe samples prepared by one-step electrochemical deposition from electrolyte at $E = -1.15$ V (Ag/AgCl electrode) (*a*) and Cu – Zn – Sn – Se precursor film (*b*).[90] The elemental compositions of samples *1* – *7* (in at.%) are shown in the upper right corner in Fig *a*.

Table 3. Main Raman lines of all possible phases that can form during the synthesis of CZT(S,Se) films.

Phase	Raman shift /cm^{-1}	Ref.
CZTS	338 – 339 (main peak), 288 – 289, 351, 368 – 373	71, 72, 91 – 95
CZTSe	194 – 197 (main peak), 171 – 173, 230 – 231, 390	71, 72, 89, 90
MoS_2	288, 384, 410 (main peak)	71, 72, 91, 93
ZnS(cubic)	352 (main peak), 275 (weak peak)	71, 72, 91, 93
Cu_2SnS_3 (tetragonal)	297, 337, 352	71, 72, 91, 93
Cu_2SnS_3 (cubic)	267, 303, 356	71, 72, 91, 93
Cu_2SnS_3 (orthogonal)	318	71, 72, 91, 93
SnS	160, 190 (main peak), 219 (orthogonal phase), 314 (hexagonal phase)	71, 72, 91, 93
$Cu_{2-x}S$	475 (main peak), 264 (weak peak)	71, 72, 91, 93
ZnSe	200, 250 – 251	71, 72, 89, 90
$MoSe_2$	168, 240, 258	71, 72, 89, 90
$Cu_{2-x}Se$	262	71, 72, 89, 90
Cu_2SnSe_3	180, 236, 251	71, 72, 89, 90
CuSe	91, 262	71, 72, 89, 90

III.4. Why the defect structure is formed

Random distribution of cations in the crystal lattice may lead to formation of point defects (vacancies and antistructural defects) and, hence, influence the electrical properties of a material. Chalcopyrite absorbers (first of all, $CuInSe_2$) were studied using various absorption and photoluminescence techniques in order to describe the electronic energy levels of point defects.[108 – 110] Clearly, the cation distribution and, especially, disorder in the Cu – Zn layer, which can induce the formation of vacancies and antistructural defects, also plays a significant role for compounds with the kesterite-type structure.

In addition, the formation of a defect structure can be due to the nonstoichiometric composition of the final Cu – Zn – Sn – (S,Se) film. However, it should be noted that nonstoichiometric composition of kesterite allows one to improve the electrical properties of a solar cell based on the kesterite absorber layer.

Various CZT(S,Se) absorber layers of different composition either enriched with or depleted in copper, zinc and tin were prepared (see, *e.g.*, Refs 70, 71, 89, 111) and their electrophysical and optical properties were studied. Measurements of the photovoltaic parameters of the samples showed that they are suitable for thin-film solar cell applications. Additional information on the influence of the defect structure of kesterites on the photovoltaic parameters of solar cells can be found in the literature.[112 – 115]

III.5. Inlfuence of secondary phases on the properties of kesterite thin films

Nonstoichiometric composition of a film can favour the formation of secondary phases, which in turn causes defect formation and thus reduces the performance of thin-film solar cells.[116 – 119] Energy defects in the semiconductor band gap serve as charge carrier traps or recombination centres. In this connection, the nature of defects in the CZT(S,Se) films and the loss of photogenerated charge carriers should be studied.

In most cases, CZT(S,Se) thin films are synthesized on molybdenum substrates; therefore, annealing in a reactive sulfur (selenium) atmosphere may lead to formation of not only the main phase, but also a molybdenum disulfide impurity phase at the Mo/CZTS interface.[23] Published data on the influence of the formation of this secondary phase on the optical and electrophysical properties of absorber layers in thin-film solar cells are contradictory.[25, 120, 121] However, changes in the lifetimes of main charge carriers, in the electron and hole trap distribution and in position of the Fermi level upon doping the main phase with impurities were confirmed in the studies of Cu(In,Ga)Se_2, CdTe and other thin films.[1, 122 – 126] In particular, the formation of a molybdenum disulfide impurity phase at the CZTS/Mo interface depends strongly on the sulfurization conditions in the course of annealing.[127] The photoconductivity of films prepared under different sulfurization conditions is related to the intensity of the main MoS_2 line in the Raman spectra of the films; the plot represents a curve with a characteristic maximum (Fig. 4). As the reduced intensity of the MoS_2 line in the Raman spectra of the CZTS film increases, the photoconductivity increases and then decreases. The maximum in the plot corresponds to optimal ratio between the secondary phase and the main phase, at which the maximum photocurrent of the CZTS film is achieved. This is in good agreement with the results obtained in a theoretical study [128] of the effect of an additional MoS_2 layer on the performance of a solar cell.

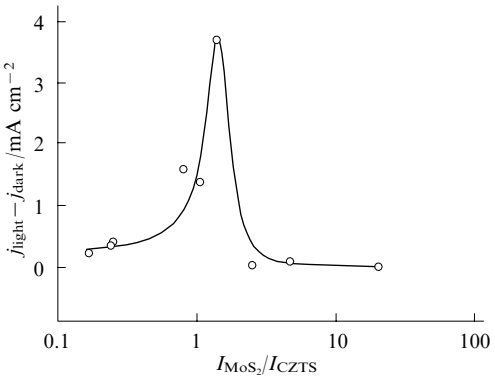


Figure 4. Photoconductivity ($j_{light} - j_{dark}$) of CZTS films prepared under different sulfurization conditions plotted *vs.* reduced intensity (I_{MoS_2}/I_{CZTS}) of the main MoS_2 line in the Raman spectra of the films.[127]
j_{light} and j_{dark} are respectively the light photoconductivity and the dark photoconductivity.

Namely, the existence of such a maximum was predicted and explained by the formation of an additional ohmic contact between the MoS_2 layer and Mo and a diode contact between the MoS_2 layer and CZTS.

IV. Electrophysical and optical properties of kesterite materials

IV.1. Band gap determination methods

Compounds Cu_2ZnSnX_4 (X = S, Se) are direct band-gap semiconductors; their E_g values are determined by analyzing the absorption spectra (Fig. 5) or reflection spectra [129, 130] using extrapolation by a straight line until the intersection with the abscissa axis. Two types of kesterite films have different band gaps, namely, ~1.50 eV (CZTS) [48, 131 – 133] and ~1.0 eV (CZTSe).[61, 90, 134, 135] The theoretical E_g value for CZTSe is ~1 eV.[136] However, for long the band gaps of kesterite semiconductor films were determined ambiguously. Table 4 lists the E_g values of CZTSe samples prepared by different methods. As can be seen, they are grouped around ~1.0 and ~1.5 eV.

The reasons for these differences are difficult to find out because the samples were prepared and the band gaps were determined using different methods; however, the following was stated with certainty:

— the value 1.5 eV was obtained from the near-red edge optical absorption spectra, whereas the value 1.0 eV was obtained by different methods (theoretical calculations, from the solar cell efficiency, and from the results of photoluminescence studies);

— most samples were analyzed only by powder X-ray diffraction; this method can be insensitive to the presence of the ZnSe and Cu_2SnSe_3 secondary phases, which can contribute to the overall E_g value.

Taking into account the aforesaid, it was concluded [136] that the main reasons for differences between the E_g values are due to either different methods used to determine the band gap or to the presence of secondary phases that can hardly be detected using powder X-ray diffraction. Subsequent analysis showed that the former reason is unlikely because all single-phase CZTSe samples were characterized by $E_g \approx 1.0$ eV irrespective of the method of determination.

An analysis of the CZTSe samples containing secondary phases revealed clear-cut differences between the E_g values of the films prepared at different substrate temperatures. This is first of all due to the fact that the content of tin decreased and the ZnSe secondary phases formed in the final samples as the substrate temperature increased. These ZnSe microinclusions are responsible for the overestimated E_g values of the CZTSe films under study.

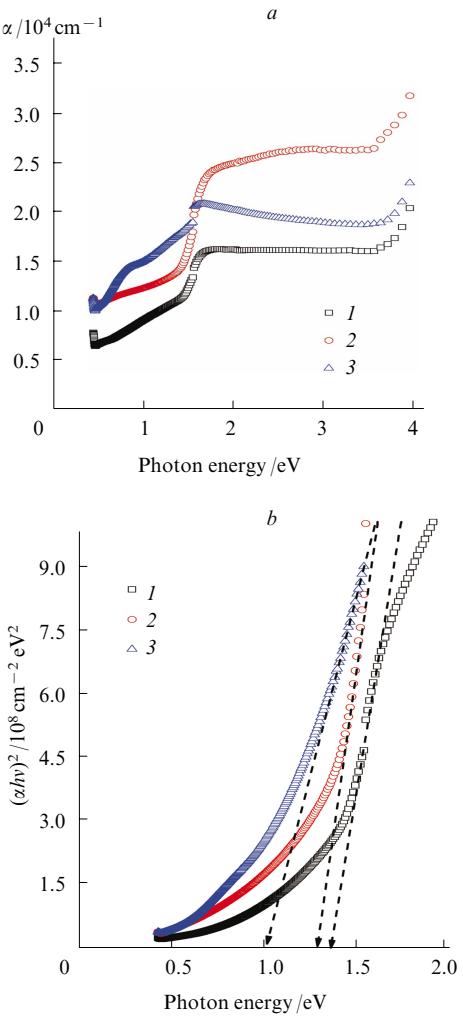


Figure 5. Absorption spectra (*a*) and an example of band gap determination (*b*) for the CZTS samples prepared by reactive sputtering of Cu, SnS_2 and ZnS targets in different order and annealed in H_2S atmosphere.[64]
Precursors were sputtered in the following order: Cu/SnS_2/ZnS/glass (*1*), ZnS/Cu/SnS_2/glass (*2*), and SnS_2/ZnS/Cu/glass (*3*); α is the absorption coefficient and *hν* is the photon energy.

Table 4. Calculated and experimentally determined E_g values in CZTSe samples.

E_g /eV	Method of synthesis of CZTSe	Method of determination of E_g	Ref.
0.8	Vacuum co-evaporation of precursors	From the solar cell efficiency	137
1.02	High-temperature synthesis from coarse-grained powder	Photoluminescence studies	138
1.0		Theoretical calculations	136, 139
0.94	Deposition of precursors followed by selenization	From the solar cell efficiency	140
1.0	Solution process using hydrazine	Optical spectroscopy	3
1.5	Vacuum co-evaporation of precursors	The same	141
1.44	High-temperature synthesis of single crystal	"	142
1.56	Radiofrequency magnetron sputtering	"	70
1.41 – 1.6	Vacuum co-evaporation of precursors	"	143

IV.2. Photoconductivity

Photoconductivity belongs to the key properties of absorber layers, which are of crucial importance for the development of thin-film solar cells. It can be studied by various contact methods including those using tailor-made electrodes as well as by contactless methods, *e.g.*, the microwave technique.

The suitability of a CZT(S,Se) absorber layer can also be assessed using fast photosensitivity tests with a photoelectrochemical cell. In many studies, kesterite films were investigated by just this method [89, 92, 94, 95, 127, 135, 144, 145] which is based on charge transfer between the photosensitive working electrode [active CZT(S,Se) sample] and the counter electrode in appropriately chosen electrolyte.

Possible electrolytes include aqueous europium nitrate [89, 92, 94, 95, 127] or sodium sulfate [135, 144] or a KOH–KI–I_2 solution.[145] In many studies, the choice of europium nitrate is quite substantiated. Europium ions, Eu^{3+}, can undergo reversible reduction to Eu^{2+} ($Eu^{3+} + e \rightleftarrows Eu^{2+}$) and thus not deposit on the cathode [(*i.e.*, the CZT(S,Se) film under study]; this facilitates measurements and introduces no errors in the experimental results. Samples placed in this electrolyte are exposed to chopped light (usually, with AM1.5 or related sources) at different potentials. Illumination of the sample produces photogenerated charge carriers to be consumed in the reduction of the Eu^{3+} ions.

If the voltage–current curve of a CZTS sample (Fig. 6) has clearly seen portions where the current density increases (light on) and decreases (light off), the sample is considered photoactive and can be used as absorber layer in thin-film solar cells. Besides, changes in the current density are suitable to determine the conductivity type of the semiconductor materials. Namely, if the photoresponse is observed in the cathodic (anodic) region, the samples exhibit p-type (n-type) conductivity. Usually, CZT(S,Se) kesterite films possess hole-type conductivity.[89, 92, 135, 144, 145]

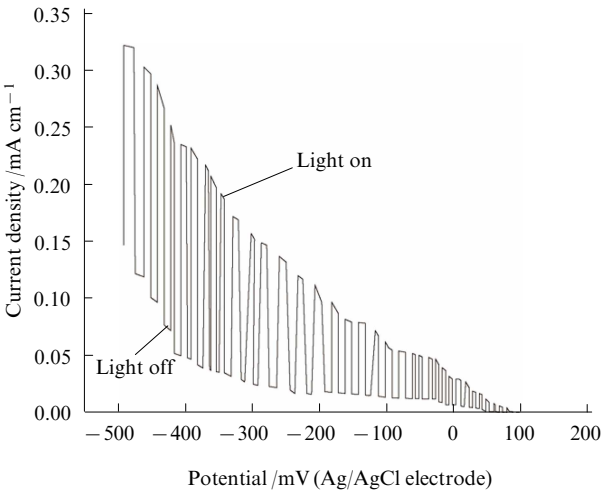


Figure 6. The voltage–current curve of a CZTS sample in a photoelectrochemical cell placed in 0.2 M aqueous $Eu(NO_3)_3$ under chopped light.[92]

IV.3. Lifetimes of photogenerated charge carriers in CZT(S,Se) films

IV.3.a. Microwave photoconductivity

Under constant illumination (best conditions for solar cell operation), the photoconductivity (σ) is given by

$$\sigma = q\,\mu_d\,n$$

where q is the elementary charge, μ_d is the drift mobility of excess (photogenerated) charge carrier, and n is the stationary concentration of charge carriers. In equilibrium, the expression for n has the form

$$n = L\,\tau$$

where L is the intensity of incident light and τ is the charge carrier lifetime determined by the carrier loss processes (recombination or trapping).

The influence of the parameter τ on the efficiency of thin-film solar cells was reported repeatedly.[146–149] For instance, the loss kinetics of photogenerated charge carriers in $Cu_{1.7}Zn_{1.1}Sn_{0.9}Se_4$ powders was studied by frequency-time-resolved microwave photoconductivity (36 GHz) with a time resolution of 5 ns.[150] The microwave photoconductivity photoresponses had very small amplitude (ΔP) and were noisy (Fig. 7 *a*).

It was found that a decrease in temperature led to an increase in the photoresponse amplitude; the characteristic decay times remained unchanged (~6 ns), being near the time resolution of the instrument. This indicates that the

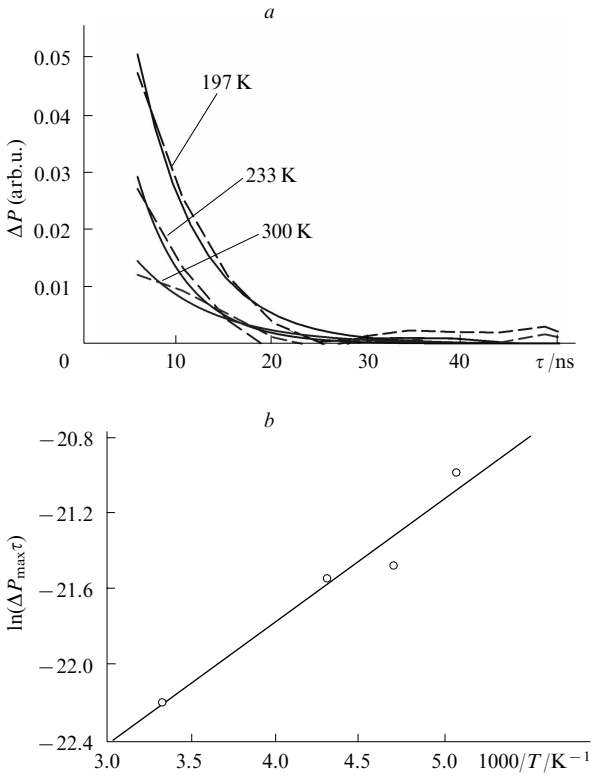


Figure 7. Microwave photoconductivity decay curves at different temperatures (dashed lines) and corresponding exponential best-fit curves (solid lines) (*a*) and the product of amplitude by the characteristic time of photoresponse decay plotted *vs.* temperature for a $Cu_{1.7}Zn_{1.1}Sn_{0.9}Se_4$ powder (*b*).[150]

lifetimes of minority charge carriers (electrons) in the kesterite films and powders were shorter than 6 ns and that the temperature dependence of the photoresponse amplitude is due to changes in the characteristic decay times. The temperature dependence of the product of amplitude by the characteristic decay time of the photoresponse plotted in the Arrhenius coordinates is shown in Fig. 7 *b*. The activation energy of electron–hole recombination estimated from this plot is $E_a \approx 54$ meV.[150]

IV.3.b. Time-resolved photoluminescence

Short lifetimes of photogenerated charge carriers were also reported in another study.[60] Based on photoluminescence data, a luminescence peak was revealed in the region 0.96 eV (1290 nm). This is reasonably close to the theoretical band gap of CZTSe equal to 1.0 eV [133] and agrees with the results obtained [136] in a joint luminescence and optical spectroscopy study.

The results of measurements are presented in Fig. 8. The decay curves were obtained at different laser power. Experimental data were fitted by the sum of two exponential curves. It was found that a decrease in the laser power causes the lifetimes to increase from 0.45 to 0.60 ns for the first component (τ_1) and from 1.65 to 2.5 ns for the second component (τ_2). This difference indicates that for kesterite materials the photoluminescence decays of both components characterize complex dynamics of processes that involve photogenerated charge carriers (mainly charge carrier recombination on the sample surface and trapping).

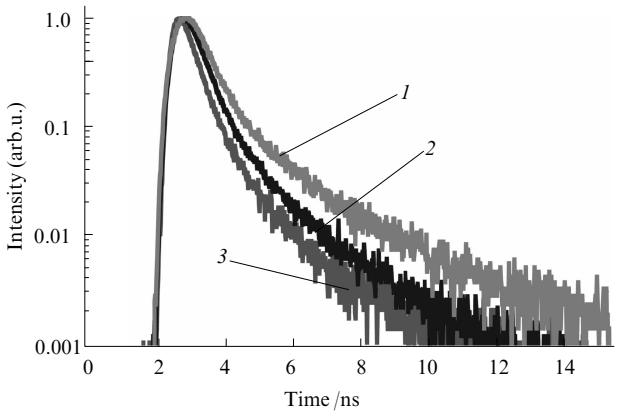


Figure 8. Time-resolved photoluminescence decay curves of a CZTSe sample at an excitation power of 0.5 (*1*), 1 (*2*) and 2 mW (*3*).[60]

The photoluminescence decay curves for CZTS samples with the kesterite structure were considered in more detail in another study [149] where the τ_2 component was ascribed to the minority carrier lifetimes and describes defects in the interior of grains and at the absorber layer/buffer layer interface and near the back contact. The τ_1 component describes high carrier injection processes in CZTS that are due to radiative recombination and redistribution of excess charge carriers near the sample surface. The charge carrier lifetimes ($\sim$10 ns) are still shorter than their lifetimes in high-performance CIGS films (200–250 ns).[151, 152]

IV.3.c. Possible reasons for short lifetimes of charge carriers in CZT(S,Se) films

Short photoluminescence decay times can be due to fast loss of charge carriers on lattice defects both in the bulk and on the surface of crystallites.

In addition, the charge carrier lifetimes can be influenced by recombination processes on point defects in the bulk of crystallites. At present, it is hard to decide between the two mechanisms. However, the size of coherent scattering regions (CSR) can indeed affect the measured microwave photoconductivity at an appropriate ratio between the drift length and the CSR size.[146–148]

Taking into account the possibility for CSR to influence the loss of charge carriers (see above), one can assume the existence of a barrier to the motion of electrons (holes) at the CSR boundaries. Nonzero activation energy for photoconductivity can also suggest that the rate constant for electron–hole recombination is temperature dependent (by analogy with the results obtained in the studies of CIGS systems [146–148] where a free electron recombined with a trapped hole).

V. Solar cells based on CZT(S,Se) kesterite films

V.1. A typical structure of a solar cell based on CZT(S,Se) films

A solar cell based on the CZT(S,Se) kesterite-type absorber layer is a complex multilayer module (Fig. 9) comprising a glass or flexible polymeric substrate, a back electrode (Mo, ITO, *etc.*), an absorber layer [CZT(S,Se) thin film], a buffer

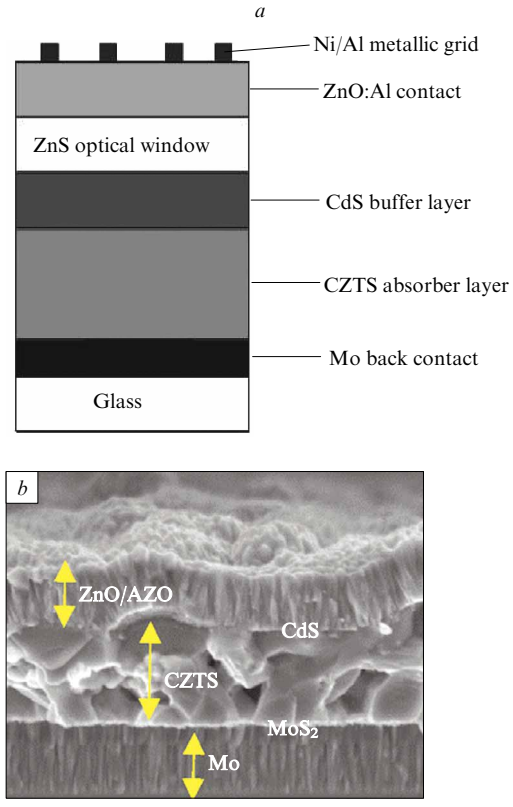


Figure 9. Multilayer structure of a solar cell based on kesterite-type CZTS absorber layer (*a*) and a photomicrograph of a cut of the solar cell (*b*).[65]

layer (CdS, ZnS or In_xS_y thin film) which forms a CZT(S,Se)/CdS heterojunction at the interface with the active layer, an optical window (ZnO, $Zn_{1-x}Mg_xO$) and a ZnO : Al upper contact. Each layer should exhibit particular properties necessary for normal operation of the solar cell.[1, 3, 15, 16, 21, 153 – 156]

V.2. Maximum power conversion efficiencies of solar cells based on CZT(S,Se) films

Although the efficiency of solar cells based on CZT(S,Se) kesterite absorber layers gradually increased in the last decade, it still remains at most 10%.

The highest PCE value of 12.6% was achieved in 2013 for a laboratory-scale sample based on mixed sulfide-selenide kesterite $Cu_2ZnSn(S,Se)_4$.[42] A PCE value of 10.1% achieved in 2012 ranks second.[157] The semiconductor material synthesized by the solution method using hydrazine was characterized by $S/(S+Se) \approx 0.4$ and $E_g = 1.15$ eV. The best result for pure CZTS film (PCE = 8.4%) was obtained in a study [158] where kesterite films were synthesized by thermal evaporation of metals *in vacuo* followed by sulfurization. The highest PCE of pure CZTSe films (9.15%) was achieved using samples prepared by co-evaporation of components onto the substrate.[60]

In other cases, the PCE of solar cells based on kesterite absorber layers was at most 6% – 7%, the lowest efficiencies being characteristic of the devices containing absorber layers synthesized by solution methods (Table 5).

The maximum efficiencies of kesterite-based thin-film solar cells were compared in a number of publications. Namely, samples prepared by CBD only,[82] those synthesized by different methods [6] and the kesterite-*vs*.-chalcopyrite-based solar cells [8] were considered.

Kesterite-based solar cells were also prepared using CZTSe powders and a CdS buffer layer in a polymer matrix.[161 – 164] However, their efficiencies were at most 5%.[163]

V.3. Why the power conversion efficiency of kesterite-based solar cells is so low

The reasons for the low PCE values of kesterite-based solar cells can be reduced to the following:[165 – 168]

— reasons related to the kesterite absorber layer and

— reasons related to the assembly of high-grade solar cells.

The efficiency of kesterite solar cells can be low owing to structural imperfection of the CZT(S,Se) absorber layer. Probably, this is related to the presence of structural defects, to deviations from the stoichiometric composition (although some authors state that nonstoichiometric compositions of the kesterite films make it possible to achieve high PCE, see, *e.g.*, Refs 27, 71, 169 – 172), to the presence of various secondary phases that also contribute to the energy properties of the CZT(S,Se) active layer, *etc*. Structural imperfections in kesterites can immediately influence recombination processes in the film, which in turn affects the lifetimes of photogenerated charge carriers. As a result, most photogenerated charge carriers recombine long before they reach the boundary of the buffer layer, thus reducing the quantum efficiency of the thin-film solar cell.

Taking into account the aforesaid, it becomes understandable why solar cells containing the CZT(S,Se) absorber layer prepared by the vacuum method are characterized by higher PCE than solar cells with the kesterite layer prepared by the solution methods (see Table 4). Namely, vacuum methods are more accurate and allow one to fabricate kesterite films of specified composition and thus exclude structural imperfections.

Also, subsequent annealing of precursor films plays a decisive role. In this step, the final kesterite-type structure is formed. In some cases, a mixture of phases [CZT(S,Se) + secondary phase] rather than pure single-phase structure can form, which will also influence the absorbing properties of the kesterite layer.[3 – 5, 7, 8, 10]

Most problems related to the assembly of high-grade solar cells can be solved by ensuring optimal contact between the CZT(S,Se) absorber layer and CdS buffer layer and other contacts, as well as by eliminating leakage current due to the presence of shunt resistance.[1, 22, 173]

VI. Conclusion

An analysis of published data presented in this review shows that quaternary copper compounds CZT(S,Se) can act as absorber layers in thin-film solar cells and become an alternative to CIGS-technology because of high natural abundance and low cost of the elements necessary to

Table 5. Power conversion efficiency of solar cells based on kesterites CZT(S,Se) prepared using different methods of synthesis of absorber layer.

Absorber layer	Method of synthesis	ζ (%)	U_{oc}/mV	j_{sc} /mA cm^{-2}	*FF* (%)	Ref.
CZTS	Magnetron sputtering of metallic targets followed by annealing in H_2S atmosphere	5.75	590	20.5	48	65
CZTS	Magnetron sputtering of Cu, SnS and ZnS targets	6.2	603	19	55	66
CZTS (flexible substrate)	Magnetron sputtering of metallic targets followed by sulfurization	3.08	491	10.6	59.2	159
CZTSSe	Magnetron sputtering of ZnS target and thermal evaporation of metallic Cu and Zn	6	390	31.5	49	63
CZTSSe	CBD	2.2	247.3	21.3	41.1	79
CZTS	Sol – gel technology	2.03	575	9.69	36.4	160
CZTS	Electrochemical synthesis	3.62	686	11.25	47	85
CZTSe	The same	4.5	307	38.81	37.4	87

Note. Notations are as follows: ζ is the power conversion efficiency, U_{oc} is the open-circuit voltage, j_{sc} is the short-circuit current density and *FF* is the fill factor.

synthesize semiconductor kesterite materials. In spite of a relatively short period of research (only 10 years), the PCE of laboratory-scale samples of the solar cells based on CZT(S,Se)/CdS heterojunctions is as high as 12.6%. This value is lower than the theoretically possible limit (30%) and the PCE of solar cells based on silicon and other thin-film materials (CdTe, CIGS); however, the results obtained give hope that kesterite materials can be used in new-generation solar cells.

It should be noted that high performance was mainly achieved using vacuum methods that are expensive and poorly scalable. An alternative is provided by rapidly developing solution methods, in particular, electrochemical deposition. This technique is readily scalable, safe and allows regeneration of the working solution. These advantages may define the prospects for application of solution methods in thin-film photovoltaics.

There has been intensive research into the photovoltaic properties of kesterite materials. Since no industrial-scale production of kesterite-based solar cells is available as yet, activity along this line can cause reduction of the cost of one Watt of the peak power produced by this type of solar cells. Thus, solar cells based on CZT(S,Se) seem to have great prospects for practical application.

The authors express their gratitude to Academician S.M.Aldoshin for inspiring discussions and for his interest in this work.

The review has been written with the financial support from the Russian Foundation for Basic Research (Project No. 16-08-01234).

References

1. G F Novikov, M V Gapanovich *Usp. Fiz. Nauk* (2017) (in the press)
2. Q Guo, G M Ford, W C Yang, B C Walker, E A Stach, H W Hillhouse, R Agrawal *J. Am. Chem. Soc.* **132** 17384 (2010)
3. T K Todorov, K B Reuter, D B Mitzi *Adv. Mater.* **22** E156 (2010)
4. H Katagiri, N Sasaguchi, S Hando, S Hoshino, J Ohashi, T Yokota *Sol. Energy Mater. Sol. Cells* **49** 407 (1997)
5. D B Mitzi, O Gunawan, T K Todorov, K Wang, S Guhaet *Sol. Energy Mater. Sol. Cells* **95** 1421 (2011)
6. H Wang *Int. J. Photoenergy* **2011** 1 (2011)
7. S Abermann *Solar Energy* **94** 37 (2013)
8. S Siebentritt *Thin Solid Films* **535** 1 (2013)
9. M Paire, S Delbos, J Vidal, N Naghavi, J F Guillemoles, in *Solar Cell Materials. Developing Technologies* (Ed. G Conibeer, A Willoughby) (London: Wiley, 2014) p. 185
10. S Delbos *EPJ Photovolt.* **3** 35004 (2012)
11. G P Bernardini, P Bonazzi, M Corazza, F Corsini, G Mazzetti, L Poggi, G Tanelli *Eur. J. Mineral.* **2** 219 (1990)
12. I V Pekov *Minerals First Discovered on the Territory of the Former Soviet Union* (Moscow: OP, 1998)
13. S Schorr, H-J Hoebler, M Tovar *Eur. J. Mineral.* **19** 65 (2007)
14. Zh I Alferov, V M Andreev, V D Rumyantsev *Semiconductors* **38** 899 (2004)
15. Zh I Alferov *Russ. Chem. Rev.* **82** 587 (2013)
16. M Meytin *Elektronika: Nauka, Tekhnologiya, Biznes* (6) 40 (2000)
17. J Lindroos, H Savin *Sol. Energy Mater. Sol. Cells* **147** 115 (2016)
18. J Plentz, G Andrä, T Pliewischkies, U Brückner, B Eisenhawer, F Falk *Mater. Sci. Eng., B* **204** 34 (2016)
19. R W Miles, G Zoppi, I Forbes *Mater. Today* **10** (11) 20 (2007)
20. T L Chu, S S Chu *Solid-State Electron.* **38** 533 (1995)
21. L A Kosyachenko *Semiconductors* **40** 710 (2006)
22. D Das, L Damodare *Mater. Chem. Phys.* **56** 48 (1998)
23. J J Scragg, P J Dale, L M Peter *Thin Solid Films* **517** 2481 (2009)
24. P K Sarswat, M Snure, M L Free, A Tiwari *Thin Solid Films* **520** 1694 (2012)
25. J Iljina, R Zhang, M Ganchev, T Raadik, O Volobujeva, M Altosaar, R Traksmaa, E Mellikov *Thin Solid Films* **537** 85 (2013)
26. W Huang, Q Li , Y Chen, Y Xia, H Huang, C Dun, Y Lin, D L Carroll *Sol. Energy Mater. Sol. Cells* **127** 188 (2014)
27. C P Chan, H Lam, C Surya *Sol. Energy Mater. Sol. Cells* **94** 207 (2010)
28. J C González, G M Ribeiro, E R Viana, P A Fernandes, P M P Salomé, K Gutiérrez, A Abelenda, F M Matinada, J P Leitão, A F da Cunha *J. Phys. D* **46** 155107 (2013)
29. W Yang, H-S Duan, K C Cha, C-J Hsu, W-C Hsu, H Zhou, B Bob, Y Yang *J. Am. Chem. Soc.* **135** 6915 (2013)
30. T Tanaka, T Nagatomo, D Kawasaki, M Nishio, Q Guo, A Wakahara, A Yoshida, H Ogawa *J. Phys. Chem. Solids* **66** 1978 (2005)
31. J Zhang, L Shao, Y Fu, E Xie *Rare Met.* **25** 315 (2006)
32. K Ito, T Nakazawa *Jpn. J. Appl. Phys.* **27** 2094 (1988)
33. Z Zhou, Y Wang, D Xu, Y Zhang *Sol. Energy Mater. Sol. Cells* **94** 2042 (2010)
34. R A Wibowo, E S Lee, B Munir, K H Kim *Phys. Status Solidi, A* **204** 3373 (2007)
35. D-H Kuo, W Wubet *J. Solid State Chem.* **215** 122 (2014)
36. D-H Kuo, M Tsega *J. Solid State Chem.* **206** 134 (2013)
37. M Tsega, D-H Kuo *Appl. Phys. Exp.* **5** 091201 (2012)
38. A Nagaoka, K Yoshino, H Taniguchi, T Taniyama, H Miyake *J. Cryst. Growth* **354** 147 (2012)
39. K Masuko, M Shigematsu, T Hashiguchi, D Fujishima, M Kai, N Yoshimura, T Yamaguchi, Y Ichihashi, T Yamanishi, T Takahama, M Taguchi, E Maruyama, S Okamoto *IEEE J. Photovolt.* **4** 1433 (2014)
40. T Matsui, H Sai, T Suezaki, M Matsumoto, K Saito, I Yoshida, M Kondo, in *Proceedings of the 28th European Photovoltaic Solar Energy Conference and Exibition, Paris, 2013* p. 2213; DOI: 10.4229/28thEUPVSEC2013-3DO.7.2
41. B M Kayes, H Nie, R Twist, S G Spruytte, F Reinhardt, I C Kizilyalli, G S Higashi, in *Proceedings of the 37th IEEE Photovoltaic Specialists Conference, Seattle, WA, 2011* p. 000004
42. W Wang, M T Winkler, O Gunawan, T Gokmen, T K Todorov, Y Zhu, D B Mitzi *Adv. Energy Mater.* **4** 1301465 (2013)
43. C Shi, G Shi, Z Chen, M Yao *Mater. Lett.* **73** 89 (2012)
44. J S Seol, S Y Lee, J C Lee, H D Nam, K H Kim *Sol. Energy Mater. Sol. Cells* **75** 155 (2003)
45. K Oishi, G Saito, K Ebina, M Nagahashi, K Jimbo, W S Maw, H Katagiri, M Yamazaki, H Araki, A Takeuchi *Thin Solid Films* **517** 1449 (2008)
46. K Moriya, K Tanaka, H Uchiki *Jpn. J. Appl. Phys.* **46** 5780 (2007)
47. K Moriya, K Tanaka, H Uchiki, *Jpn. J. Appl. Phys.* **47** 602 (2008)

48. H Katagiri, K Saitoh, T Washio, H Shinohara, T Kurumadani, S Miyajima *Sol. Energy Mater. Sol. Cells* **65** 141 (2001)
49. N Kamoun, H Bouzouita, B Rezig *Thin Solid Films* **515** 5949 (2007)
50. Y B K Kumar, G S Babu, P U Bhaskar, V S Raja *Sol. Energy Mater. Sol. Cells* **93** 1230 (2009)
51. K Tanaka, M Oonuki, N Moritake, H Uchiki *Sol. Energy Mater. Sol. Cells* **93** 583 (2009)
52. G L Agawane, A S Kamble, S A Vanalakar, S W Shin, G Gang, J H Yun, J Gwak, A V Moholkar, J H Kim *Mater, Lett.* **158** 58 (2015)
53. X Zhang, X Shi, W Ye, C Ma, C Wang *Appl. Phys. A: Mater. Sci. Proc.* **94** 381 (2009)
54. S Ji, C Ye *Rev. Adv. Sci. Eng.* **1** (1) 42 (2012)
55. K Ramasamy, M A Malik, P O'Brien *Chem. Commun. (Cambridge)* **48** 5703 (2012)
56. H R Jung, S W Shin, K V Gurav, M P Suryawanshi, C W Hong, H S Yang, J Y Lee, J H Moon, J H Kim *Ceram. Int.* **41** 13006 (2015)
57. A Alvarez, S Exarhos, L Mangolini *Mater. Lett.* **165** 41 (2016)
58. T S Shyju, S Anandhi, R Suriakarthick, R Gopalakrishnan, P Kuppusami *J. Solid State Chem.* **227** 165 (2015)
59. Y-P Lin, Y-F Chi, T-E Hsieh, Y-C Chen, K-P Huang *J. Alloys Compd.* **654** 498 (2016)
60. I Repins, C Beall, N Vora, C DeHart, D Kuciauskas, P Dippo, B To, J Mann, W-C Hsu, A Goodrich, R Noufi *Sol. Energy Mater. Sol. Cells* **101** 154 (2012)
61. O Volobujeva, J Raudoja, E Mellikov *J. Phys. Chem. Solids* **70** 567 (2009)
62. S Jung, J Gwak, J H Yun, S J Ahn, D Nam, H Cheong, S Ahn, A Cho, K S Shin, K H Yoon *Thin Solid Films* **535** 52 (2013)
63. L Grenet, S Bernardi, D Kohen,Ch Lepoittekin, S Noël, N Karst, A Brioude, S Perraud, H Mariette *Sol. Energy Mater. Sol. Cells* **101** 11 (2012)
64. S W Shin, S M Pawar, C Y Park, J H Yun, J H Moon, J H Kim, J Y Lee *Sol. Energy Mater. Sol. Cells,* **95** 3202 (2011)
65. A Emrani, P Vasekar, Ch R Westgate *Solar Energy* **98** 335 (2013)
66. T P Dhakal, C-Y Peng, R R Tobias, R Dasharathy, Ch R Westgate *Solar Energy* **100** 23 (2014)
67. S M Pawar, A I Inamdar, K V Gurav, S W Shin, Y Jo, J Kim, H Im, J H Kim *Vacuum* **104** 57 (2014)
68. A I Inamdar, S Lee, K-Y Jeon, Ch H Lee, S M Pawar, R S Kalubarme, Ch J Park, H Im, W Jung, H Kim *Solar Energy* **91** 196 (2013)
69. B-T Jheng, K-M Huang, S-F Chen, M-C Wu *Thin Solid Films* **564** 345 (2014)
70. R A Wibowo, W S Kim, E S Lee, B Munir, K H Kim *J. Phys. Chem. Solids* **68** 1908 (2007)
71. A Fairbrother, X Fontane, V Izquierdo-Roca, M Espíndola-Rodríguez, S López-Marino, M Placidi, L Calvo-Barrio, A Pérez-Rodríguez, E Saucedo *Sol. Energy Mater. Sol. Cells* **112** 97 (2013)
72. R B V Chalapathy, G S Jung, B T Ahn *Sol. Energy Mater. Sol. Cells* **95** 3216 (2011)
73. H Katagiri, K Jimbo, S Yamada, T Kamimura, W S Maw, T Fukano, T Ito, T Motohiro *Appl. Phys. Exp.,* **1** 041201 (2008)
74. K Wang, O Gunawan, T Todorov, B Shin, S J Chey, N A Bojarczuk, D Mitzi, S Guha *Appl. Phys. Lett.* **97** 143508 (2010)
75. T S Tlemçani, El Bachir Benamar, F Ch El Moursli, F Hajji, Z Edfouf, M Taibi, H Labrim, B Belhorma, S Aazou, G Schmerber, K Bouras, Z Sekkat, A Dinia, A Ulyashin, A Slaoui *Energy Proc.* **84** 127 (2015)
76. S Shin, Ch Park, Ch Kim, Y Kim, S Park, J-H Lee *Curr. Appl. Phys.* **16** 207 (2016)
77. S K Aditha, A D Kurdekar, L A A Chunduri, S Patnaik, V Kamisetti *MethodsX* **3** 35 (2016)
78. T R Rana, N M Shinde, J H Kim *Mater. Lett.* **162** 40 (2016)
79. H Dong, Th Schnabel, E Ahlswede, C Feldmann *Solid State Sci.* **29** 52 (2014)
80. A Wangperawong, J S King, S M Herron, B P Tran, K Pangan-Okimoto, S F Bent *Thin Solid Films* **519** 2488 (2011)
81. M Zhou, Ya Gong, J Xu, G Fang, Q Xu, J Dong *J. Alloys Compd.* **574** 272 (2013)
82. Y E Romanyuk, C M Fella, A R Uhl, M Werner, A N Tiwari, T Schnabel, E Ahlswede *Sol. Energy Mater. Sol. Cells,* **119** 181 (2013)
83. M Cao, L Li, B L Zhang, J Huang, L J Wang, Y Shen, Y Sun, J C Jiang, G J Hu *Sol. Energy Mater. Sol. Cells* **117** 81 (2013)
84. Q Zhang, M Cao, W Sh Gao, J Yang, J Sh Shen, J Huang, Y Sun, L J Wang, Y Shen *Mater. Des.* **91** 37 (2016)
85. Y Li, T Yuan, L Jiang, Zh Su, F Liu *J. Alloys Compd.* **610** 331 (2014)
86. R Juskenas, S Kanapeckaite, V Karpaviciene, Z Mockus, V Pakstas, A Selskiene, R Giraitis, G Niaura *Sol. Energy Mater. Sol. Cells* **101** 277 (2012)
87. Y Zhang, C Liao, K Zong, H Wang, J B Liu, T Jiang, J F Han, G Q Liu, L Cui, Q Y Ye, H Yan, W M Lau *Solar Energy* **94** 1 (2013)
88. J Li, T Ma, M Wei, W Liu, G Jiang, Ch Zhu *Appl. Surface Sci.* **258** 6261 (2012)
89. W Septina, Sh Ikeda, A Kyoraiseki, T Harada, M Matsumura *Electrochim. Acta* **88** 436 (2013)
90. M Meng, L Wan, P Zou, Sh Miao, J Xu *Appl. Surface Sci.* **273** 613 (2013)
91. M Jeon, T Shimizu, S Shingubara, *Mater. Lett.* **65** 2364 (2011)
92. S M Pawar, B S Pawar, A V Moholkar, D S Choi, J H Yun, J H Moon, S S Kolekar, J H Kim *Electrochim. Acta* **55** 4057 (2010)
93. M Jeon, Y Tanaka, T Shimizu, S Shingubara *Energy Proc.* **10** 255 (2011)
94. V V Rakitin, M V Gapanovich, P A Mikhailov, I A Domashnev, A M Kolesnikova, G F Novikov *Kondensirovannye Sredy i Mezhfaznye Granitsy* **15** 312 (2013)
95. V V Rakitin, M V Gapanovich, G F Novikov *Mendeleev Commun.* **24** 9 (2014)
96. S Schorr *Sol. Energy Mater. Sol. Cells* **95** 1482 (2011)
97. A Khare, B Himmetoglu, M Johnson, D J Norris, M Cococcioni, E S Aydil *J. Appl. Phys.* **111** 083707 (2012)
98. C Persson *J. Appl. Phys.* **107** 053710 1 (2010)
99. S R Hall, J T Szymanski, J M Stewart *Canad. Mineral.* **16** 131 (1978)
100. L O Brockway *Z. Kristallogr.* **89** 434 (1934)
101. P Bonazzi, L Bindi, G P Bernardini, S Menchetti *Can. Miner.* **41** 639 (2003)

102. I D Olekseyuk, L D Gulay, I V Dydchak, L V Piskach, O V Parasyuk, O V Marchuk *J. Alloys Compd.*, **340** 141 (2002)
103. S Chen, X G Gong *Phys. Rev. B* **79** 165211-1 (2009)
104. S Siebentritt, S Schorr *Prog. Photovolt.: Res. Appl.* **20** 512 (2012)
105. T Wada, S Nakamura, T Maeda *Prog. Photovolt.: Res. Appl.* **20** 520 (2012)
106. B G Mendis, M D Shannon, M C J Goodman, J D Major, R Claridge, D P Halliday, K Durose *Prog. Photovolt.: Res. Appl.* **22** 24 (2014)
107. H Nozaki, T Fukano, S Ohta, Y Seno, H Katagiri, K Jimbo *J. Alloys Compd.* **524** 22 (2012)
108. A L Li, I Shih *J. Electron. Mater.* **22** 195 (1993)
109. A M Bakry, A M Elnaggar *J. Mater. Sci., Mater. Electron.* **7** 191 (1996)
110. G Zahn, P Paufler *Cryst. Res. Technol.* **23** 499 (1988)
111. R A Wibowo, H Yoo, A Holzing, R Lechner, S Jost, J Palm, M Gowtham, B Louis, R Hock *Tin Solid Films* **535** 57 (2013)
112. E Kask, T Raadik, M Grossberg, R Josepson, J Krustok *Energy Proc.* **10** 261 (2011)
113. A Nagaoka, K Yoshino, H Taniguchi, T Taniyama, H Miyake *J. Cryst. Growth* **341** 38 (2012)
114. T Washio, H Nozaki, T Fukano, T Motohiro, K Jimbo, H Katagiri *J. Appl. Phys.* **110** 074511 (2011)
115. I Repins, N Vora, C Beall, S H Wei, Y Yan, M Romero, G Teeter, H Du, B To, M Young, R Noufi, in *Presented at the Materials Research Society Spring Meeting, San Francisco, 2011* p. 14
116. A Redinger, D M Berg, P J Dale, N Valle, S Siebentritt *J. Photovolt.* **1** 200 (2011)
117. A-J Cheng, M Manno, A Khare, C Leighton, S A Campbell, E S Aydil *J. Vac. Sci. Technol. A* **29** 051203 (2011)
118. A Redinger, D M Berg, P J Dale, S Siebentritt *J. Am. Chem. Soc.* **133** 3320 (2011)
119. A Ennaoui, M Lux-Steiner, A Weber, D Abou-Ras, I Kötschau, H-W Schock, R Schurr, A Holzing, S Jost, R Hock, T Voy, J Schulze, A Kirbs *Thin Solid Films* **517** 2511 (2009)
120. W Li, J Chen, H Cui, F Liu, X Hao *Mater. Lett.* **130** 87 (2014)
121. M P Suryawanshi, S W Shin, U V Ghorpade, K V Gurav, G L Agawane, Ch W Hong, J H Yun, P S Patil, J H Kim, A V Moholkar *Solar Energy* **110** 221 (2014)
122. E V Rabenok, M V Gapanovich, G F Novikov, I N Odin *Semiconductors* **43** 846 (2009)
123. M V Gapanovich, K V Bocharov, G F Novikov *J. Renew. Sust. Energy* **5** 011201 (2013)
124. M V Gapanovich, N A Radychev, E V Rabenok, D N Voilov, I N Odin, G F Novikov *High Energy Chem.* **41** 126 (2007)
125. M V Gapanovich, N A Radychev, E V Rabenok, D N Voilov, I N Odin, G F Novikov *Inorg. Mater.* **43** 1065 (2007)
126. G F Novikov, E V Rabenok, M J Jeng, L B Chang. *J. Renew. Sust. Energy* **4** 011604 (2012)
127. V V Rakitin, M V Gapanovich, G F Novikov *Russ. Chem. Bull., Int. Ed. (Engl. Transl.)* **11** 2586 (2015)
128. P Chelvanathan, M I Hossain, J Husna, M Alghoul, K Sopian, N Amin *Jpn. J. Appl. Phys.* **51** 10NC32 (2012)
129. Yu V Meteleva, G F Novikov *Semiconductors,* **40** 1137 (2006)
130. X Mathew, P J Sebastian *Sol. Energy Mater. Sol. Cells* **59** 85 (1999)
131. B Schubert, B Marsen, S Cinque, T Unold, R Klenk, S Schorr, H-W Schock *Prog. Photovolt.: Res. Appl.,* **19** 93 (2011)
132. T M Friedlmeier, H Dittrich, H W Schock *J. Phys., Conf. Ser.,* **152** 345 (1998)
133. S Chen, A Walsh, J-H Yang, X Gong, L Sun, P-X Yang, J-H Chu, S-H Wei *Phys. Rev. B: Condens. Matter.* **83** 125201 (2011)
134. B Ananthoju, F J Sonia, A Kushwaha, D Bahadur, N V Medhekar, M Aslam *Electrochim. Acta* **137** 154 (2014)
135. M Farinella, R Inguanta, T Spanò, P Livreri, S Piazza, C Sunseri *Energy Proc.* **44** 105 (2014)
136. S J Ahn, S Jung, J Gwak, A Cho, K Shin, K Yoon, D Park, H Cheong, J H Yun *Appl. Phys. Lett.* **97** 021905-1 (2010)
137. T M Friedlmeier, N Wieser, T Walter, H Dittrich, H W Schock, in *Proceedings of the 14th European Photovoltaic Specialists Conference, Barcelona, 1997* p. 1242
138. M Grossberg, J Krustok, K Timmo, M Altosaar *Thin Solid Films* **517** 2489 (2009)
139. S Chen, X G Gong, A Walsh, S H Wei *Appl. Phys. Lett* **94** 041903 (2009)
140. G Zoppi, I Forbes, R W Miles, P J Dale, J J Scragg, L M Peter *Prog. Photovolt.* **17** 315 (2009)
141. G S Babu, Y B K Kumar, P U Bhaskar, V S Raja *J. Phys. D: Appl. Phys* **41** 205305 (2008)
142. H Matsushita, T Maeda, A Katsui, T Takizawa *J. Cryst. Growth* **208** 416 (2000)
143. G S Babu, Y B K Kumar, P U Bhaskar, S R Vanjari *Sol. Energy Mater. Sol. Cells* **94** 221 (2010)
144. G Ma, T Minegishi, D Yokoyama, J Kubota, K Domen *Chem. Phys. Lett.,* **501** 619 (2011)
145. N M Shinde, C D Lokhande, J H Kim, J H Moon *J. Photochem. Photobiol., A* **235** 14 (2012)
146. K V Bocharov, G F Novikov, T Y Hsieh, M V Gapanovich, M J Jeng *Semiconductors* **47** 335 (2013)
147. G Novikov, K Bocharov, T Y Hsieh, M J Jeng, in *Proceedings of the 27th European Photovoltaic Solar Energy Conference & Exibition (27th EU PVSEC), Frankfurt, 2012* p. 2851
148. M J Jeng, K Bocharov, T Y Hsieh, G Novikov, in *Proceedings of the 22nd International Photovoltaic Science and Engineering Conference (PVSEC-22), Hangzhou, China, 2012* p. 3
149. O Gunawan, T K Todorov, D B Mitzi *Appl. Phys. Lett.,* **97** 233506 (2010)
150. M Gapanovich, G Novikov, K Bocharov, W-T Tsai, M-J Jeng, L-B Chang *The 23rd Photovoltaic Science and Engineering Conference (PVSEC-23) Taiwan, China, 2013* http://www.pvsec23.com/conf_news.html
151. W K Metzger, I L Repins, M A Contreras *Appl. Phys. Lett.* **93** 022110 (2008)
152. I L Repins, W K Metzger, C L Perkins, J V Li, M A Contreras *IEEE Transact. Electron Dev.*, **57** 2957 (2010)
153. M Patel, A Ray *Physica B: Condens. Matter* **407** 4391 (2012)
154. N Sakai, H Hiroi, H Sugimoto in *Proceedings of the 37th IEEE Photovoltaic Specialists Conference, Seattle, WA, 2011* p. 003654
155. F Jiang, H Shen,W Wang, L Zhang *Appl. Phys. Expr.* **4** 074101 (2011)
156. P K Sarswat, M L Free *Phys. Status Solidi A* **208** 2861 (2011)
157. D A R Barkhouse, O Gunawan, T Gokmen, T K Todorov, D B Mitzi *Prog. Photovolt.: Res. Appl.* **20** 6 (2012)
158. B Shin, O Gunawan, Y Zhu, N A Bojarczuk, S J Chey, S Guha, *Prog. Photovolt.: Res. Appl.* **21** 72 (2013)

159. Ch-Y Peng, T P Dhakal, S Garner, P Cimo, S Lu, Ch R Westgate *Thin Solid Films,* **562** 574 (2014)
160. K Tanaka, Yu Fukui, N Moritake, H Uchiki *Sol. Energy Mater. Sol. Cells* **95** 838 (2011)
161. K Muska, M Kauk, M Grossberg, J Raudoja, O Volobujeva *Energy Proc.* **10** 323 (2011)
162. E Mellikov, M Altosaar, M Krunks, J Krustok, T Varema, O Volobujeva, M Grossberg, L Kaupmees, T Dedova, K Timmo, K Ernits, J Kois, I Oja Acik, M Danilson, S Bereznev *Thin Solid Films* **516** 7125 (2008)
163. M Kauk-Kuusik, M Altosaar, K Muska, M Pilvet, J Raudoja, K Timmo, T Varema, M Grossberg, E Mellikov, O Volobujeva *Thin Solid Films* **535** 18 (2013)
164. E Mellikov, D Meissner, T Varema, M Altosaar, M Kauk, O Volobujeva, J Raudoja, K Timmo, M Danilson *Sol. Energy Mater. Sol. Cells* **93** 65 (2009)
165. J M Raulot, C Domain, J F Guillemoles *J. Phys. Chem. Solids* **66** 2019 (2005)
166. A Opanasyuk, D Kurbatov, M Ivashchenko, I Y Protsenko, H Cheong *J. Nano-Electron. Phys.* **4** (1) 01024 (2012)
167. B Shin, Y Zhu, N A Bojarczuk, S J Chey, S Guha *App. Phys. Lett.* **101** 053903 (2012)
168. S Bag, O Gunawan, T Gokmen, Y Zhu, T K Todorov, D B Mitzi *Energy Environ. Sci.* **5** 7060 (2012)
169. J J Scragg, P J Dale, L M Peter, G Zoppi, I Forbes *Phys. Status Solidi B* **245** 1772 (2008**)**
170. X Fontaner, L Calvo-Barrio, V Izquierdo-Roca, E Saucedo, A Perrez-Rodriguez, J R Morante, D M Berg, P J Dale, S Siebentritt *Appl. Phys. Lett.* **98** 181905 (2011)
171. A Fairbrother, E García-Hemme, V Izquierdo-Roca, X Fontané, F A Pulgarín-Agudelo, O Vigil-Galán, A Pérez-Rodríguez, E Saucedo *J. Am. Chem. Soc.* **134** 8018 (2012)
172. A Nagoya, R Asahi, G Kreese *J. Phys.: Condens. Matter* **23** 404203 (2011)
173. N M Shinde, P R Deshmukh, S V Patil, C D Lokhande *Mater. Res. Bull.* **48** 1760 (2013)